Chapter 4

A Closed-Loop Coherent PN Acquisition Scheme for Direct-Sequence Spread-Spectrum Systems Using a New Auxiliary Sequence

4.1 Introduction

In Chapter 3, the closed-loop PN acquisition of Salih and Tantaratana [26] is modified for the noncoherent demodulator. The proposed noncoherent scheme still uses the same auxiliary signal as [26]. The simulation results show that the proposed noncoherent scheme acquires the correct phase faster than the conventional noncoherent serial search scheme.

The auxiliary signal is designed so that its cross-correlation with the PN signal is a triangular shape spanning the whole period of NT_c as shown in Figure 3.2. Due to the triangular cross-correlation, the search direction can be adjusted by inspecting the cross-correlation of the incoming PN signal with the advance and delayed versions of the auxiliary signal. However, a disadvantage of the auxiliary signal is that it has large range of values, which requires more storage and longer processing time. For example, the auxiliary signal generated from the PN signal with polynomial $h(x) = 1 + x^3 + x^7$, i.e. $N=127$, is plotted in Figure 4.1. We see that the value spans from -300 to 350.

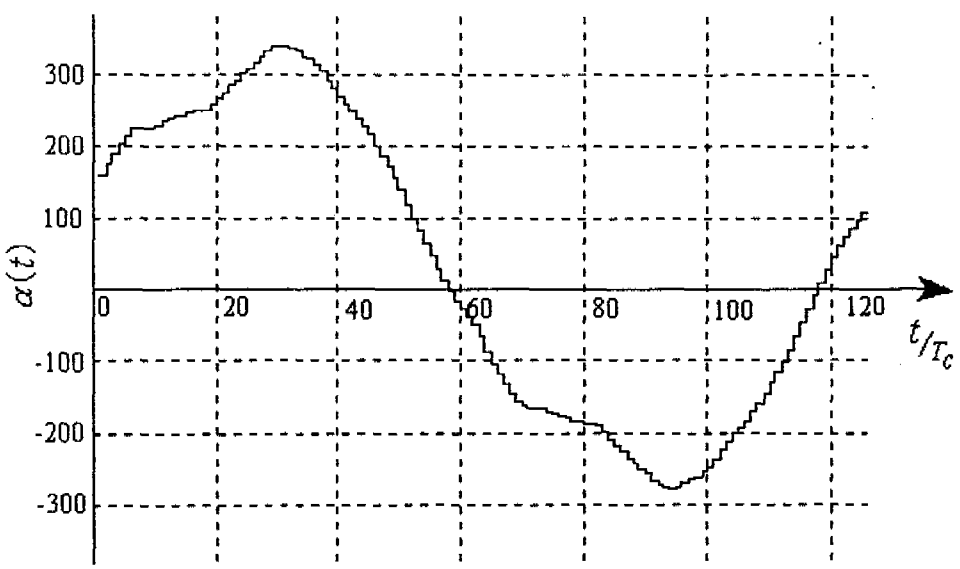

Figure 4.1: Waveform of the auxiliary signal used in [26] where $N=127$

To simplify the closed-loop in [26], the auxiliary signal $\alpha(t)$ generator, delay, and summation can be reduce to be a signal $x(t)$ generator where

$$x(t) = \alpha\left(t - \frac{T_c}{2}\right) - \alpha\left(t + \frac{T_c}{2}\right). \tag{4.1}$$

The signal $x(t)$ can be formed directly from the PN sequence. Let it be called "an auxiliary signal $x_d(t)$" where d is a number of stable point when it is applied to a VCC loop. In the first case $d = 1$, i.e. $x(t)$ in (4.1) $= x_1(t)$, the auxiliary signal yields

$$x_1(t) = \sum_{i=1}^{\frac{N-1}{2}} \left[c(t - iT_c + \tfrac{T_c}{2}) - c(t + iT_c - \tfrac{T_c}{2})\right]. \tag{4.2}$$

It is plotted in Figure 4.2. Comparing to those of Figure 4.1, we see that peak-to-peak values has been significantly reduced.

In this chapter we propose a new auxiliary signal and an acquisition scheme using a new auxiliary signal. Section 4.2 describes the detail of the proposed scheme. In Section 4.3 the probabilities of detection and false alarm are derived. Section 4.4 presents some simulation results.

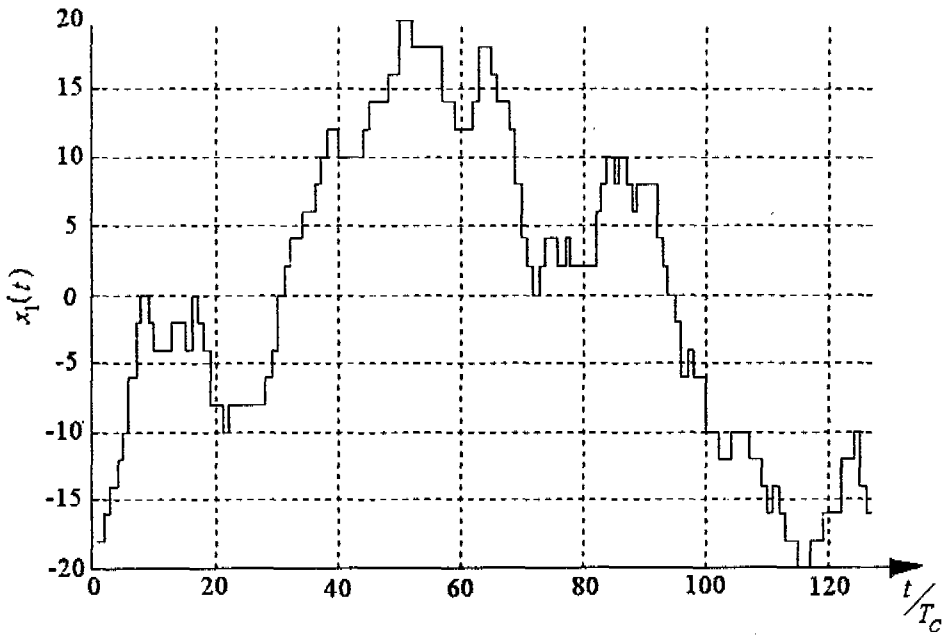

Figure 4.2: Waveform of a signal $x_1(t)$ where $N = 127$

4.2 The Proposed Coherent Scheme

During PN acquisition, the DS/SS signal arrived at the receiver consists of the signal part and noise part, which can be written as (3.1). Assume that the carrier phase is known so that the acquisition system uses coherent carrier demodulator. Let the equivalent baseband signal of (3.1) be $v(t)$, which is written as

$$v(t) = \sqrt{2P}c(t-\tau) + z(t) \tag{4.3}$$

where $z(t)$ is a zero mean white Gaussian process with PSD $2N_0$ as same as (3.3). Note that θ of (3.1) does not appear in (4.3) since coherent demodulation is assumed. Let the phase of the local PN signal be $\hat{\tau}$ and the phase error be (3.4). Without loss of generality, we may write the phase error as

$$e_\tau = (j+\gamma)T_c \tag{4.4}$$

where j is an integer and $-0.5 < \gamma \le 0.5$ so that γT_c is the fractional portion.

We propose the new auxiliary which makes the VCC loop have 2 stables points. In this section we describe the characteristic of the auxiliary signal and the proposed coherent scheme, which is separated into the VCC loop and the phase alignment detector.

4.2.1 New Auxiliary Signal $x_2(t)$

The new auxiliary signal $x_2(t)$ is defined as

$$x_2(t) = \sum_{i=1}^{\frac{N-3}{4}} [c(t-iT_c) - c(t-iT_c)] - \sum_{i=\frac{N+1}{4}}^{\frac{N-1}{2}} [c(t-iT_c) - c(t+iT_c)]. \tag{4.5}$$

Its wave form is shown in Figure 4.3 for an m-sequences c_k generated by the polynomial $h(x) = 1 + x^3 + x^7$, i.e., N =127. A method for designing the auxiliary signal is described in Appendix C. The cross-correlation of (4.5) and the PN signal $c(t)$ can be shown to be

$$\begin{aligned} R_{cx_2}(\beta) &= \frac{1}{NT_c}\int_0^{NT_c} c(t+\beta)x_2(t)dt \\ &= \begin{cases} -\frac{N+1}{NT_c}\beta, & |\beta| \\ -\operatorname{sgn}(\beta)\frac{N+1}{N}, & T_c \le |\beta| \le \frac{N-3}{4}T_c \\ 2\operatorname{sgn}(\beta)\frac{N+1}{NT_c}\left(|\beta| - \frac{N-1}{4}T_c\right), & \frac{N-3}{4}T_c < |\beta| < \frac{N+1}{4}T_c, \\ \operatorname{sgn}(\beta)\frac{N+1}{N}, & \frac{N+1}{4}T_c \le |\beta| \le \frac{N-1}{2}T_c \\ 2\operatorname{sgn}(\beta)\frac{N+1}{N}\left(\frac{NT_c}{2} - |\beta|\right), & \frac{N-1}{2}T_c < |\beta| \le \frac{N}{2}T_c \end{cases} \end{aligned} \tag{4.6}$$

which is plotted in Figure 4.4. The cross-correlation function is a periodic function with period NT_c, i.e. $R_{cx_2}(\beta) = R_{cx_2}(\beta + NT_c)$. We see that each period of the cross-correlation cover all of the PN signal phase.

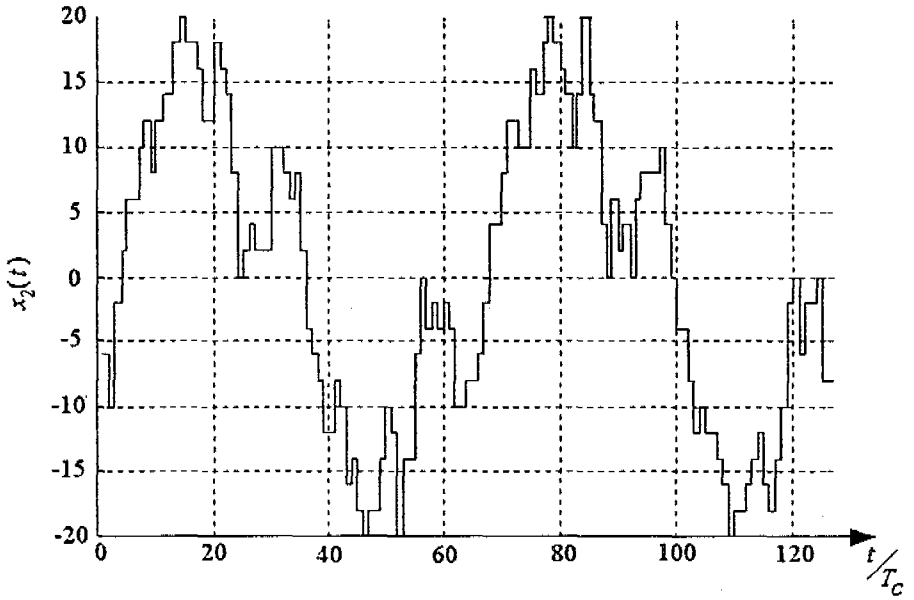

Figure 4.3: The new auxiliary signal waveform where N =127

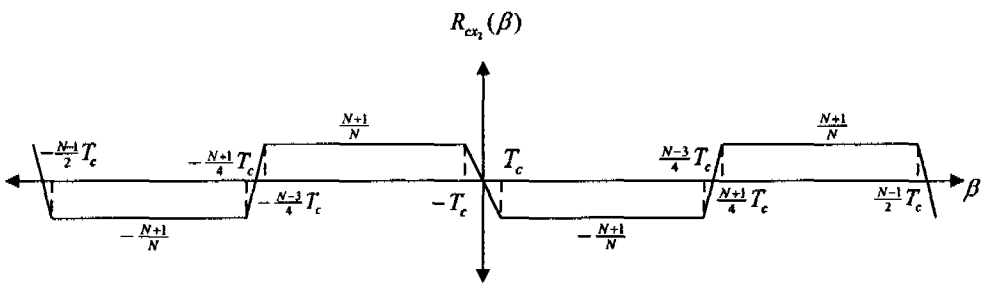

Figure 4.4: The periodic cross-correlation $R_{cx_2}(\beta)$

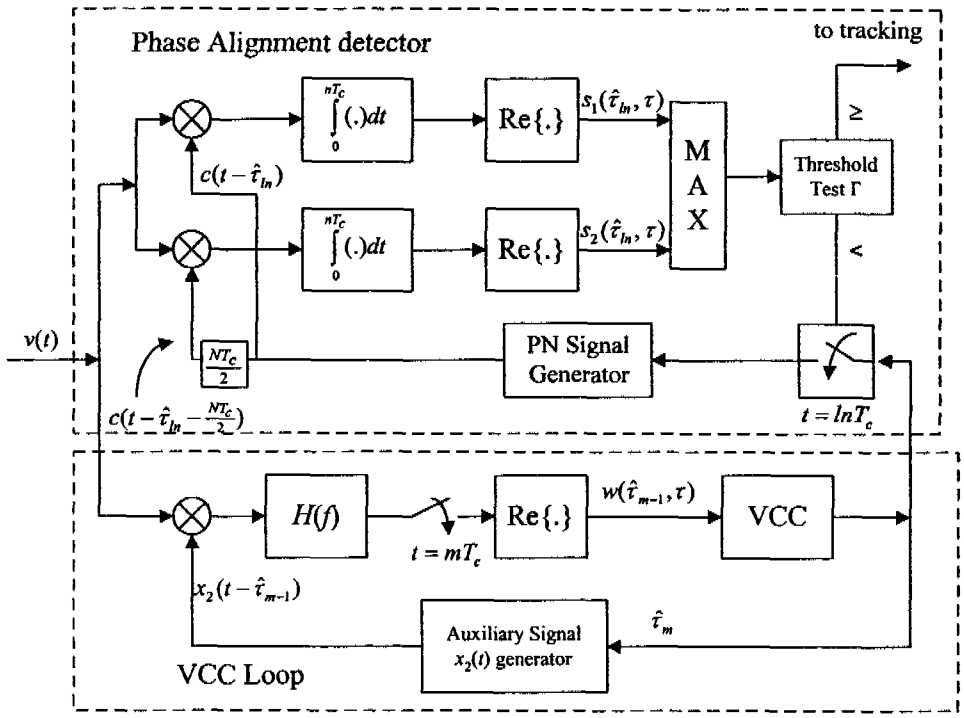

Figure 4.5: The proposed coherent scheme

4.2.2 VCC Loop

The proposed PN acquisition scheme is shown in Figure 4.5. It consists of a VCC loop and a phase alignment detector. The VCC loop is the lower part of Figure 4.5. Its function is to control the phase updating of the PN signal by adjusting the phase of the auxiliary signal toward the correct phase.

The VCC loop consists of an auxiliary signal generator, a real part operator, a VCC, and a correlator. The correlator consists of a multiplier and a filter $H(f)$ which is defined as (3.11). We now describe how the VCC loop works.

The auxiliary signal $x_2(t)$ is correlated with the incoming signal $v(t)$ and sampled at $t = mT_c$ where $m \in \{1,2,3,...\}$. The sampled signal at mT_c is

$$\begin{aligned} w(\hat{\tau}_{m-1},\tau) &= \frac{1}{M}\mathrm{Re}\left\{\int_{(m-M)T_c}^{mT_c} v(t)x_2(t-\hat{\tau}_{m-1})dt\right. \\ &= \frac{1}{M}\mathrm{Re}\left\{\sum_{k=m-M}^{m-1}\int_{kT_c}^{(k+1)T_c}\left[\sqrt{2P}c(t-\tau)+z(t)\right]x_2(t-\hat{\tau}_k)dt\right\} \\ &= \frac{\sqrt{2P}T_c}{M}\sum_{k=m-M}^{m-1}\left[q_{k+1}(\hat{\tau}_k,\tau)+\eta_{k+1}\right] \end{aligned} \tag{4.7}$$

where $\hat{\tau}_k$ is the phase of the auxiliary signal at $(m-1)T_c$, $q_{k+1}(\hat{\tau}_k,\tau)$ and η_{k+1} are given as

$$q_{k+1}(\hat{\tau}_k,\tau)=\frac{1}{T_c}\int_{kT_c}^{(k+1)T_c} c(t-\tau)x_2(t-\hat{\tau}_k)dt \tag{4.8}$$

$$\eta_{k+1}=\frac{1}{\sqrt{2PT_c}}\int_{kT_c}^{(k+1)T_c} z_R(t)x_2(t-\hat{\tau}_k)dt\,. \tag{4.9}$$

The signal $w(\hat{\tau}_{m-1},\tau)$ is the error signal which controls the VCC loop. The VCC produces an estimate $\hat{\tau}_m$ at mT_c using the following formula

$$\hat{\tau}_m=\hat{\tau}_{m-1}+K_{VCC}w(\hat{\tau}_{m-1},\tau) \tag{4.10}$$

where K_{VCC} is a constant which must be properly chosen.

The signal $w(\hat{\tau}_{m-1},\tau)$ is a random variable. From (4.7) η_m is a noise term which is a zero-mean Gaussian random variable with variance

$$\sigma^2_{\eta_{k+1}}=\frac{1}{SNR}\left[(0.5+\gamma_k)x^2_{2,k-1-j_k}+(0.5-\gamma_k)x^2_{2,k-j_k}\right] \tag{4.11}$$

where j_k and γ_k are j and γ at $t=kT_c$, $(k=m+1)$. Therefore, the average signal of w for a phase error e_τ is as follows

$$\begin{aligned}\overline{w}&=\frac{1}{N}\sum_{m=0}^{N-1}\mathrm{E}_{\eta_m}\left[w(\hat{\tau}_{m-1},\tau)\right]\\&=\frac{1}{N}\sum_{m=0}^{N-1}\mathrm{E}_{\eta_m}\left[\frac{\sqrt{2PT_c}}{M}\sum_{k=m-M}^{m-1}\left[q_{k+1}(\hat{\tau}_k,\tau)+\eta_{k+1}\right]\right]\\&=\frac{\sqrt{2PT_c}}{MN}\sum_{m=0}^{N-1}\sum_{k=m-M}^{m-1}q_{k+1}(\hat{\tau}_k,\tau)\\&=\sqrt{2PT_c}R_{cx_2}(e_\tau)\end{aligned} \tag{4.12}$$

which is shown in Figure 4.6. $E_{\eta_m}\{.\}$ is the statistical expectation with respect to noise η_m. Note that (4.12) is the delay discriminator characteristic of the VCC loop. It has 2 stable points and its pull-in range is $\frac{NT_c}{4}$. The stable points of the VCC loop are at $e_\tau=0$ and $e_\tau=\frac{NT_c}{2}$.

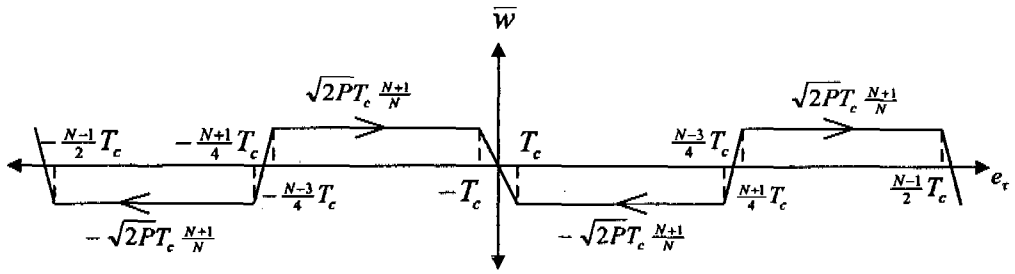

Figure 4.6: The VCC loop discriminator characteristic

4.2.3 Phase Alignment Detector

The upper part of Figure 4.5 is the phase alignment detector. Due to the two stable points of the VCC loop, the phase alignment detector needs to distinguish these two points. Therefore, it has two signal processing branches, as shown in Figure 4.5. Each branch consists of a correlator and a real part operator. The larger signal from the two parts is selected by the maximum selector (MAX), and the result is compared to a threshold.

The phase of the PN signal is supplied by the VCC loop, which is updated at $t = lnT_c$ where $l \in \{1,2,3,...\}$ and n is the integration length. Note that in the VCC loop the phase of the auxiliary signal is updated every T_c; but in the phase alignment, the PN signal phase is updated only every nT_c. To avoid jumping over the correct phase, the amount of each phase update should not be larger than T_c. Thus, from (4.10) we select K_{VCC} such that

$$\left|nK_{VCC}w(\hat{\tau}_{m-1},\tau)\right| \le T_c \tag{4.13}$$

Substituting $w(\hat{\tau}_{m-1},\tau)$ by the maximum of its mean (from Figure 4.6) yields

$$K_{VCC} \le \frac{N}{n\sqrt{2P}(N+1)} \tag{4.14}$$

On the other hand, a small K_{VCC} shows down the time to reach acquisition. Therefore, we choose the value on the right-hand side of (4.14) for the constant K_{VCC}.

For analysis purpose, we can model the alignment test as a choice between the following two hypotheses:

$$\begin{aligned} H_1 &: \left|e_\tau\right| \le \tfrac{T_c}{2} \text{ or } \tfrac{N-1}{2} \le \left|e_\tau\right| \le \tfrac{NT_c}{2} \quad \text{(alignment)} \\ H_0 &: T_c \le \left|e_\tau\right| \le \tfrac{N-2}{2}T_c \qquad\qquad \text{(no alignment)} \end{aligned} \tag{4.15}$$

The case when $\frac{T_c}{2} < |e_\tau| < T_c$ and $\frac{N-2}{2}T_c < |e_\tau| < \frac{N-1}{2}T_c$ are not included because we want to keep some distance between the sets included in H_1 and H_0. If they are included in either H_1 or H_0, then it will be very difficult to distinguish the two hypotheses from each other, resulting in an unreasonable system design and poor performance. Writing e_τ in terms of j and γ as defined in (4.4), the two hypotheses H_1 and H_0 can be expressed as

$$\begin{aligned}
H_1: \quad & j = 0 \quad \text{and} \quad -0.5 < \gamma \le 0.5 \\
& \text{or } j = -1 \quad \text{and} \quad \gamma = 0.5 \\
& \text{or } j = \tfrac{N-1}{2} \quad \text{and} \quad 0 \le \gamma \le 0.5 \\
& \text{or } j = -\tfrac{N-1}{2} \quad \text{and} \quad -0.5 < \gamma \le 0 \\
H_0: \quad & j \in I = \left\{\tfrac{-N+3}{2}, \tfrac{-N+5}{2}, \ldots, -3, -2, 2, 3, \ldots, \tfrac{N-5}{2}, \tfrac{N-3}{2}\right\} \text{ and } -0.5 < \gamma \le 0.5 \\
& \text{or } j = \tfrac{-N+1}{2} \quad \text{and} \quad \gamma = 0.5 \\
& \text{or } j = -1 \quad \text{and} \quad -0.5 < \gamma \le 0 \\
& \text{or } j = 1 \quad \text{and} \quad 0 \le \gamma \le 0.5.
\end{aligned} \tag{4.16}$$

The values of the correlation of duration nT_c and the threshold Γ of the phase alignment detector are obtained from the desired detection probability P_d and the false alarm probability P_{fa}. A good acquisition system should have appropriate choices of P_d and P_{fa}. In the next section we obtain expressions for P_d and P_{fa}.

4.3 Probabilities of Detection and False Alarm

Detection probability is the probability that the phase alignment is declared when H_1 is true. The phase alignment must chooses the correct signal between $s_1(\hat{\tau}_{ln}, \tau)$ and $s_2(\hat{\tau}_{ln}, \tau)$. Referring to Figure 4.5, these signals are

$$s_1(\hat{\tau}_{ln}, \tau) = \int_0^{nT_c} c(t - \hat{\tau}_{ln}) c(t - \tau) dt + \int_0^{nT_c} c(t - \hat{\tau}_{ln}) z_R(t) dt \tag{4.17}$$

and

$$s_2(\hat{\tau}_{ln}, \tau) = \int_0^{nT_c} c(t - \hat{\tau}_{ln} - \tfrac{NT_c}{2}) c(t - \tau) dt + \int_0^{nT_c} c(t - \hat{\tau}_{ln} - \tfrac{NT_c}{2}) z_R(t) dt \tag{4.18}$$

where $\hat{\tau}_{ln}$ is the local PN signal phase at $t = lnT_c$. The second terms of these equations are noise terms, which are zero-mean Gaussian random variables with the same variance of

$$\sigma_{s_1}^2 = \sigma_{s_2}^2 = nN_0T_c. \tag{4.19}$$

Phase alignment detection can occur in two situations. First, given that $|e_\tau| \le \frac{T_c}{2}$, we obtain detection when the event A_1 is true, where

$$A_1 = \{s_1(\hat{\tau}_{ln}, \tau) > s_2(\hat{\tau}_{ln}, \tau)\} \cap \{s_1(\hat{\tau}_{ln}, \tau) > \Gamma\}. \tag{4.20}$$

The second case of detection occurs when A_2 is true given that $\frac{N-1}{2}T_c \le |e_\tau| \le \frac{NT_c}{2}$, where

$$A_2 = \{s_2(\hat{\tau}_{ln}, \tau) > s_1(\hat{\tau}_{ln}, \tau)\} \cap \{s_2(\hat{\tau}_{ln}, \tau) > \Gamma\}. \tag{4.21}$$

The probability of detection is the weighted value of the probabilities in these two cases. Letting $B_1 = \left\{|e_\tau \le \frac{T_c}{2}\right|$ and $B_2 = \left\{\frac{N-1}{2}T_c \le |e_\tau| \le \frac{NT_c}{2}\right.$, we have

$$P_d = \frac{\Pr(A_1|B_1)\Pr(B_1) + \Pr(A_2|B_2)\Pr(B_2)}{\Pr(B_1) + \Pr(B_2)}. \tag{4.22}$$

Assuming that e_τ is equally likely to be any where in [0, NT_c], we have $\Pr(B_1) = \Pr(B_2) = 1/N$ and

$$P_d = \frac{\Pr(A_1|B_1) + \Pr(A_2|B_2)}{2}. \tag{4.23}$$

The correlation coefficient ρ of $s_1(\hat{\tau}_{ln}, \tau)$ and $s_2(\hat{\tau}_{ln}, \tau)$ is

$$\begin{aligned} \rho &= \frac{E\{s_1(\hat{\tau}_{ln}, \tau)s_2(\hat{\tau}_{ln}, \tau)\}}{\sigma_{s_1}\sigma_{s_2}} \\ &= \frac{1}{nT_c}\int_0^{nT_c} c(t-\tau)c(t-\tau-\tfrac{NT_c}{2})dt \\ &\approx 0. \end{aligned} \tag{4.24}$$

Therefore, we may assume that $s_1(\hat{\tau}_{ln}, \tau)$ and $s_2(\hat{\tau}_{ln}, \tau)$ are uncorrelated. Since they are jointly Gaussian, they are also statistically independent and their joint probability density function (pdf) is the product of their individual pdf's, i.e.,

$$f_{s_1 s_2}(x, y) = f_{s_1}(x) f_{s_2}(y). \tag{4.25}$$

Letting $s_1' = s_1(\hat{\tau}_{ln}, \tau)/\left(\sqrt{2PT_c}\right)$ and $s_2' = s_2(\hat{\tau}_{ln}, \tau)/\left(\sqrt{2PT_c}\right)$, the pdf's of s_1' and s_2' are

$$f_{s_1'}(x \mid j,\gamma) = \left(\frac{SNR}{2n\pi}\right)^{1/2} e^{SNR[x-\lambda(n,\gamma,j)]^2/2n}, \quad -\infty < x < \infty \tag{4.26}$$

$$f_{s_2'}(y \mid j,\gamma) = \left(\frac{SNR}{2n\pi}\right)^{1/2} e^{SNR\left[y-\lambda(n,\gamma-\frac{\mathrm{sgn}(\gamma)}{2},j+\frac{N+\mathrm{sgn}(\gamma)}{2})\right]^2/2n}, \quad -\infty < y < \infty \tag{4.27}$$

and

$$f_{s_1's_2'}(x,y \mid j,\gamma) = f_{s_1'}(x \mid j,\gamma) f_{s_2'}(y \mid j,\gamma) \quad -\infty < x,y < \infty \tag{4.28}$$

where

$$\lambda(n,\gamma,j) = (1-|\gamma|)\sum_{k=0}^{n-1} c_k c_{k-j} + |\gamma|\sum_{k=0}^{n-1} c_k c_{k-j-\mathrm{sgn}(\gamma)}. \tag{4.29}$$

The worst-case detection probability occurs when e_τ is half a chip off from either one of the stable points, i.e., when $e_\tau = 0.5T_c$ ($j = 0$, $\gamma = 0.5$) or $e_\tau = -\frac{N-1}{2}T_c$ ($j = -\frac{N-1}{2}T_c, \gamma = 0$). Thus the worst-case P_d is

$$P_d = \frac{1}{2}\left[\int_{\Gamma'}^{\infty}\int_{-\infty}^{x} f_{s_1's_2'}(x,y \mid 0,0.5)dydx + \int_{\Gamma'}^{\infty}\int_{-\infty}^{x} f_{s_1's_2'}(x,y \mid -(N-1)/2,0)dxdy\right] \tag{4.30}$$

where $\Gamma' = \Gamma/(\sqrt{2PT_c})$. Substituting (4.26) and (4.27) into (4.30), the two terms are equal, so we have

$$\begin{aligned} P_d &= \int_{\Gamma'}^{\infty}\int_{-\infty}^{x} f_{s_1's_2'}(x,y \mid 0,0.5)dydx \\ &= \left(\frac{SNR}{2n\pi}\right)^{1/2}\int_{\Gamma'}^{\infty} e^{-\frac{SNR[x-\lambda(n,0.5,0)]}{2n}} \Phi\left(\frac{x-\lambda(n,0,\frac{N+1}{2})}{\sqrt{n/SNR}}\right)dx \end{aligned} \tag{4.31}$$

where $\Phi(x)$ is the cdf of the standard Gaussian random variable given by

$$\Phi(x) = \frac{1}{\sqrt{2\pi}}\int_{-\infty}^{x} e^{-\frac{\xi}{2}}d\xi. \tag{4.32}$$

The false alarm probability is the probability of accepting H_1 given that H_0 is true. When false alarm occurs, the tracking circuit loses some time trying to track the wrong phase. The time spent until the tracking circuit realizes that it cannot track is called penalty time. In this thesis, we assume the penalty time to be a multiple of nT_c

which is defined as (3.43). The false alarm probability is the average probability over the range of e_τ under H_0, as given by (4.16), i.e.,

$$P_{fa} = \frac{1}{(N-4)T_c} \int_{T_c \le |e_\tau| \le \left(\frac{N-2}{2}\right)T_c} \Pr[\text{accept } H_1 \mid e_\tau] de_\tau \tag{4.33}$$

Because $e_\tau = (j+\gamma)T_c$, we write $\Pr[\text{accept } H_1 \mid e_\tau]$ as

$$\begin{aligned} \Pr[\text{accept } H_1 \mid j,\gamma] &= 1 - \Pr[s_1 < \Gamma, s_2 < \Gamma] \\ &= 1 - \left[\int_{-\infty}^{\Gamma} f_{s_1}(x \mid j,\gamma)dx\right]\left[\int_{-\infty}^{\Gamma} f_{s_2}(y \mid j,\gamma)dy\right] \end{aligned} \tag{4.34}$$

Substituting (4.34) into (4.33) yields

$$\begin{aligned} P_{fa} = 1 - \frac{1}{N-4}\Bigg\{ & \sum_{j\in I}\left[\int_{-0.5}^{0.5} \Phi\left(\frac{\Gamma' - \lambda(n,\gamma,j)}{\sqrt{n/SNR}}\right)\Phi\left(\frac{\Gamma' - \lambda\left(n,\gamma - \frac{\text{sgn}(\gamma)}{2}, j + \frac{N+\text{sgn}(\gamma)}{2}\right)}{\sqrt{n/SNR}}\right)d\gamma\right] \\ & + \int_{-0.5}^{0} \Phi\left(\frac{\Gamma' - \lambda(n,\gamma,-1)}{\sqrt{n/SNR}}\right)\Phi\left(\frac{\Gamma' - \lambda\left(n,\gamma+0.5,\frac{N-1}{2}\right)}{\sqrt{n/SNR}}\right)d\gamma \\ & + \int_{0}^{0.5} \Phi\left(\frac{\Gamma' - \lambda(n,\gamma,1)}{\sqrt{n/SNR}}\right)\Phi\left(\frac{\Gamma' - \lambda\left(n,\gamma+0.5,\frac{N+3}{2}\right)}{\sqrt{n/SNR}}\right)d\gamma\Bigg\}. \end{aligned} \tag{4.35}$$

Given the desired values of P_d and P_{fa}, the value of n and can be computed numerically from (4.31) and (4.35).

4.4 Simulation Results

We use simulation to investigate the performance of the proposed scheme. Note that the acquisition time of a PN acquisition system is the time from the start until the PN phase is correctly acquired. In the simulation we obtain the mean acquisition time and the variance of the acquisition time. A flowchart of the simulation program is depicted in Figure 4.7 where K is the number of trails.

As in Chapter 3, four cases of simulation were carried out with the parameters given in Table 4.1. In Case 1 and Case 2, we can compare the effect of parameter K_p. For Case 1 and Case 3, we can compare the effect of P_d and P_{fa}. Case 1 and Case 4, the effect of *SNR* on the proposed scheme can be compared. The PN sequence used in the simulation is an m-sequence with polynomial $h(x) = 1 + x^4 + x^9$, i.e. $N = 511$. In each case, the length M of the filter $H(f)$ is varied from 500 to 7500 and K =2555. The results for the proposed scheme are shown in Figures 4.8 and 4.9. Figure 4.8 is the mean acquisition time of the proposed scheme. As expected, the mean acquisition time for -5 dB is higher than that for 0 dB. If K_p increases, the mean acquisition time also increases. However, it changes slightly as M changes. Figure 4.9 depicts the variance of the acquisition time of the proposed scheme.

Table 4.1:
Parameter values used in the simulation of the proposed coherent scheme and performance of the conventional scheme

Case	*SNR* (dB)	P_{fa}	P_d	Correlation duration		K_p	Conventional scheme performance	
				Proposed scheme(n)	Conventional Scheme(n')		Mean of acq. time /T_c	Variance of acq. time / $(1{,}000T_c)^2$
1	-5	0.1	0.9	98	87	20	69,913	6,821
2	-5	0.1	0.9	98	87	60	115,093	19,959
3	-5	0.05	0.95	112	97	20	67,114	6,777
4	0	0.05	0.95	50	46	20	31,337	619

The performance of the proposed scheme is compared with the conventional coherent serial scheme which is shown in Figure 2.1. The mean and variance of the acquisition time of the conventional scheme are given in Table 4.1. Comparison results are shown in Figures 4.10 and 4.11 where the two ratios R_1 and R_2 are defined as

$$R_1 = \frac{\overline{T}_{\text{co,serial}}}{\overline{T}_{\text{co,close}}} \tag{4.36}$$

where $\overline{T}_{\text{co,serial}}$ is the mean acquisition time of the conventional serial search scheme and $\overline{T}_{\text{co,close}}$ is the mean acquisition time of the proposed scheme, and

$$R_2 = \frac{\sigma^2_{\text{co,serial}}}{\sigma^2_{\text{co,close}}} \tag{4.37}$$

where $\sigma^2_{\text{co,serial}}$ is the variance of the acquisition time of the conventional scheme and $\sigma^2_{\text{co,close}}$ is the variance of the acquisition time of the proposed scheme. From both Figures 4.9 and 4.10, we see that the proposed scheme acquires the phase three to four times faster than the conventional scheme with a variance smaller than that of the conventional scheme by 10 to 40 times.

The closed-loop acquisition scheme proposed in [26] acquires the PN phase approximately 2-2.5 times faster than the conventional scheme. Therefore, our proposed scheme is about 1.5 time faster than the scheme in [26], at the expense of a slight increase of hardware, i.e., one more correlator in the phase alignment detector and a comparator (MAX operation).

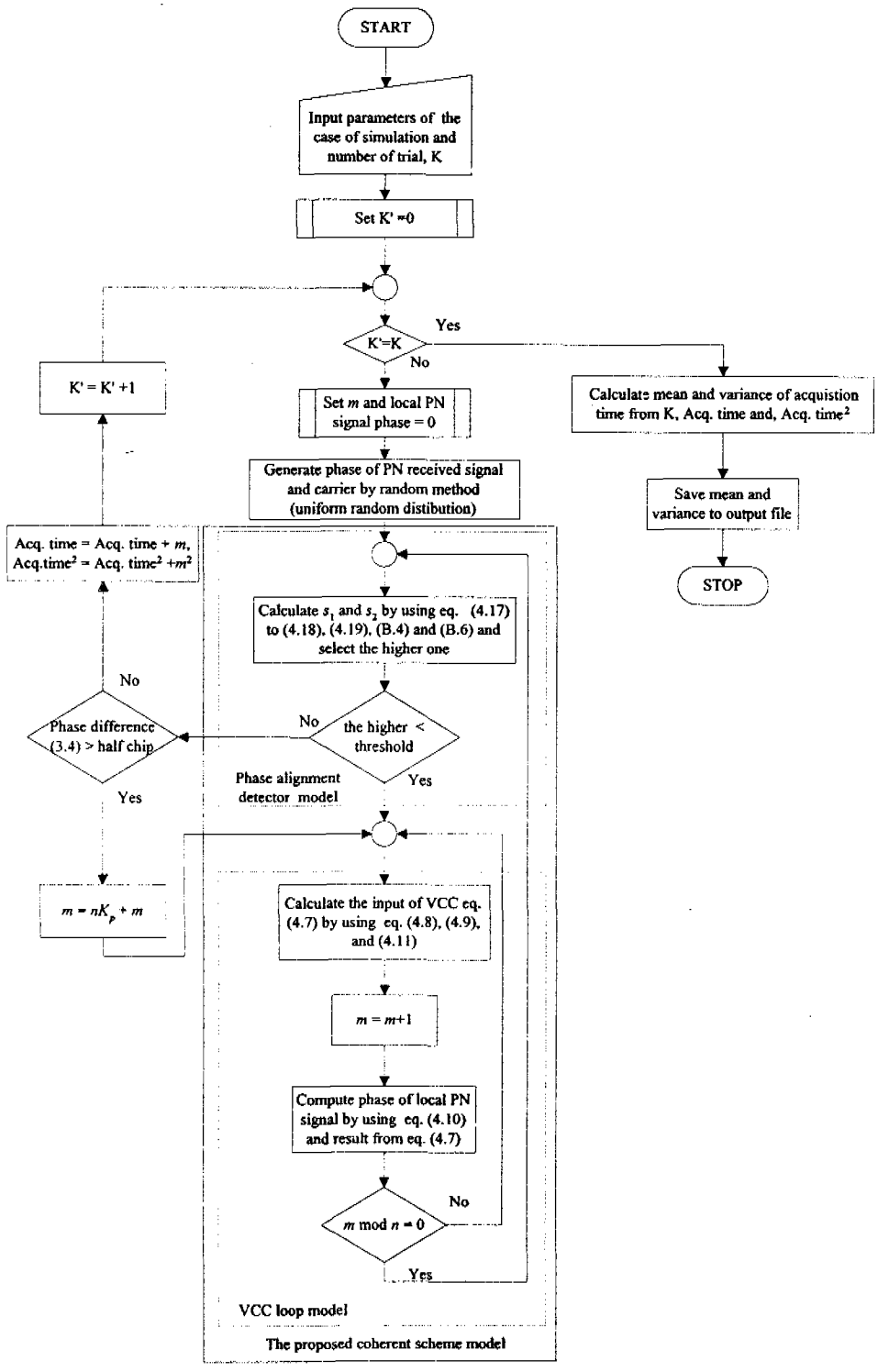

Figure 4.7: Flowchart of the simulation program for the proposed coherent scheme

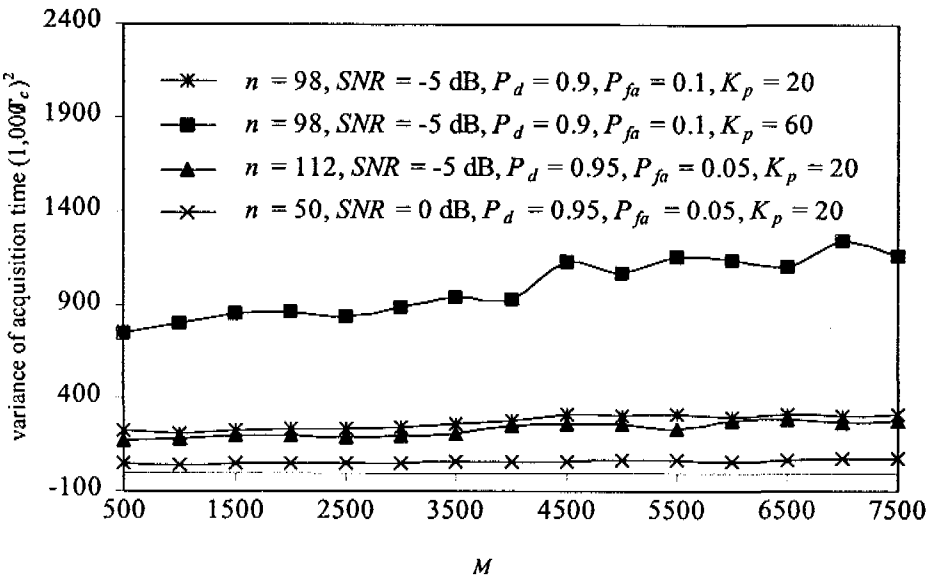

Figure 4.8: Variance of the acquisition time of the proposed coherent scheme

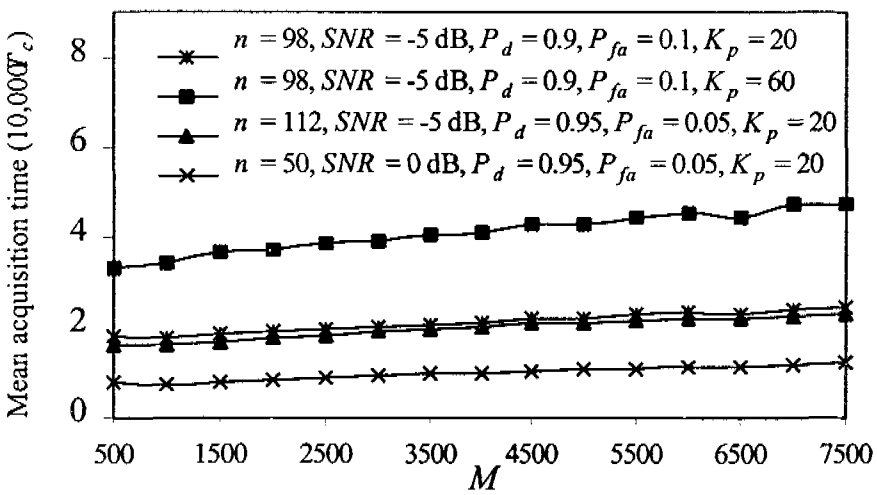

Figure 4.7: Mean acquisition time of the proposed coherent scheme

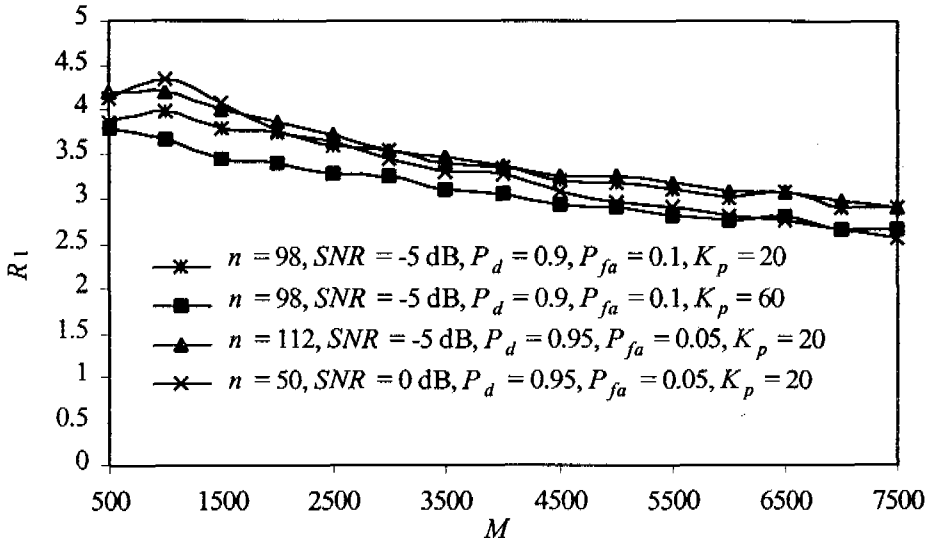

Figure 4.9: Ratio of the mean acquisition time of the conventional coherent serial scheme to that of the proposed scheme

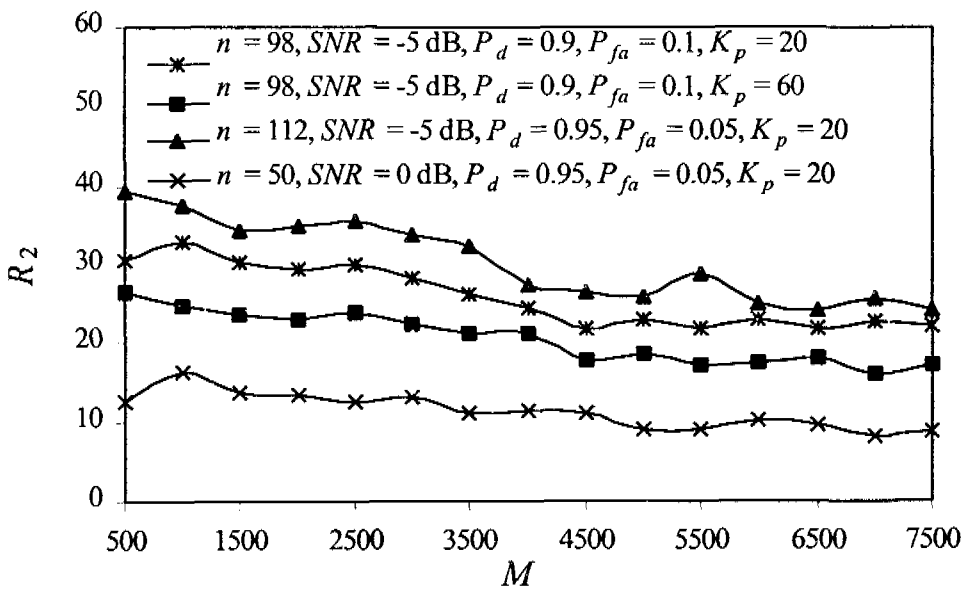

Figure 4.10: Ratio of the variance of the acquisition time of the conventional coherent serial scheme to that of the proposed scheme